The N-Terminal Extension of Cardiac Troponin T Stabilizes the Blocked State of Cardiac Thin Filament

Sampath K. Gollapudi, Ranganath Mamidi, Sri Lakshmi Mallampalli, and Murali Chandra*
Department of Veterinary and Comparative Anatomy, Pharmacology, and Physiology, Washington State University, Pullman, Washington

ABSTRACT Cardiac troponin T (cTnT) is a key component of contractile regulatory proteins. cTnT is characterized by a ~32 amino acid N-terminal extension (NTE), the function of which remains unknown. To understand its function, we generated a transgenic (TG) mouse line that expressed a recombinant chimeric cTnT in which the NTE of mouse cTnT was removed by replacing its 1–73 residues with the corresponding 1–41 residues of mouse fast skeletal TnT. Detergent-skinned papillary muscle fibers from non-TG (NTG) and TG mouse hearts were used to measure tension, ATPase activity, Ca^{2+} sensitivity (pCa_{50}) of tension, rate of tension redevelopment, dynamic muscle fiber stiffness, and maximal fiber shortening velocity at sarcomere lengths (SLs) of 1.9 and 2.3 μm. Ca^{2+} sensitivity increased significantly in TG fibers at both short SL (pCa_{50} of 5.96 vs. 5.62 in NTG fibers) and long SL (pCa_{50} of 6.10 vs. 5.76 in NTG fibers). Maximal cross-bridge turnover and detachment kinetics were unaltered in TG fibers. Our data suggest that the NTE constrains cardiac thin filament activation such that the transition of the thin filament from the blocked to the closed state becomes less responsive to Ca^{2+}. Our finding has implications regarding the effect of tissue- and disease-related changes in cTnT isoforms on cardiac muscle function.

INTRODUCTION

Troponin T (TnT) is important for the Ca^{2+}-mediated regulation of striated thin filaments. TnT structurally bridges the thin-filament proteins troponin C, troponin I, and tropomyosin (Tm). Thus, TnT plays a pivotal role in Ca^{2+}-mediated activation of thin filaments. Although previous studies have suggested that the sequence heterogeneity between cardiac TnT (cTnT), fast skeletal TnT (fsTnT), and slow skeletal TnT underlie some functional differences among different muscle types (1–3), the biological significance of the N-terminal extension (NTE) of cTnT remains unknown. A striking feature of the N-terminus of cTnT is that it has a distinct extended region that is absent in fsTnT and slow skeletal TnT. The NTE of cTnT is unique for two main reasons: 1), it is approximated by a length of 32 amino acids that are rich in negative charge; and 2), it is highly conserved in hearts of different species. Thus, the unique features of this 32 amino acid extended region of cTnT suggest that it plays an important cardiac-specific functional role (1–5).

To define the functional role of sequence differences between cTnT and fsTnT, previous studies used in vitro methods to reconstitute recombinant proteins into detergent-skinned muscle fiber preparations (5–7). These in vitro studies suggested that the amino acids 1–76 (5), 1–96 (6), or 1–91 (7) of cTnT are important for Ca^{2+}-activated force and ATPase activity of cardiac myofilaments. Although these studies (5–7) suggested a functional role for the N-terminal region of cTnT, the specific functional significance of the NTE in cTnT remains unresolved. Given that this 32 amino acid extension is highly conserved in hearts of different species, it is essential to understand its function in the heart. Other previous attempts to address the functional differences between cTnT and fsTnT employed a transgenic (TG) mouse approach in which the chicken fsTnT was overexpressed in the mouse heart (8–10). Although these TG mouse studies provided useful information, the specific role of the NTE could not be addressed because of major sequence differences in the central and the C-terminal regions of chicken fsTnT and mouse cTnT (McTnT).

The main objective of our study was to understand the functional role that is specific to the NTE in cTnT. We hypothesized that the cardiac-specific NTE has a unique regulatory role in the Ca^{2+}-mediated regulation of cardiac myofilament activation. To test our hypothesis, we made selective alterations within the N-terminal end of McTnT while conserving other regions, so that the functional differences could be solely attributed to the NTE. To our knowledge, this is the first TG mouse study that explicitly addresses the biological significance of the NTE in cTnT. We generated a TG mouse line that expressed a chimeric cTnT isoform in which 1–73 amino acids of McTnT were replaced with the corresponding 1–41 residues of mouse fsTnT (MfsTnT). The expression level of the chimeric cTnT was ~54% in TG mouse hearts. Detergent-skinned papillary muscle fiber bundles from non-TG (NTG) and TG mouse hearts were used to measure isometric tension, ATPase activity, myofilament Ca^{2+} sensitivity, rate of tension redevelopment, dynamic muscle fiber stiffness, and maximal muscle fiber shortening velocity at short (1.9 μm) and long (2.3 μm) sarcomere lengths (SLs). We discuss these data in terms of the constraining effect of the cardiac NTE on the blocked-to-closed-state transition of the thin filament during Ca^{2+}-mediated myofilament activation.

Submitted April 26, 2012, and accepted for publication July 9, 2012.

*Correspondence: murali@vetmed.wsu.edu

Editor: K.W. Ranatunga.

0006-3495/12/09/0940/9 $2.00

http://dx.doi.org/10.1016/j.bpj.2012.07.035

MATERIALS AND METHODS

Animal protocols

All mice used in this study received proper care and treatment in accordance with the guidelines set by the Washington State University Institutional Animal Care and Use Committee. NTG and TG mice were housed in individual cages and treated alike.

Generation of TG mice expressing chimeric cTnT

DNA mutagenesis was used to create a mouse chimeric cTnT gene containing nucleotides that encode 1–41 amino acids of MfsTnT gene and 74–288 residues of McTnT. The chimeric gene was then subcloned into the *Sal*I-*Hin*dIII site of the plasmid pBS2K+. The accuracy of the ligated gene sequence in the plasmid was verified by sequencing. TG mice were generated by microinjection of the DNA according to a previously described protocol (11). PCR was used to identify the founder mice as described previously (12). Breeding of the founder mice with NTG FVBN mice was set up to verify that the founder mice were able to transmit the chimeric gene to subsequent generation of offspring. After four generations, a stable TG line was obtained by breeding a female founder mouse with its NTG FVBN cohort male.

Determination of expression levels and phosphorylation status of sarcomeric proteins in NTG and TG cardiac muscle preparations

To better resolve the separation between various sarcomeric proteins, we ran a standard 8% SDS-PAGE (see Fig. S1 *A* in the Supporting Material) and a large 12.5% SDS-PAGE (Fig. S1 *B*) after loading the gels with equal quantities of the digested muscle protein extracts from NTG and TG mouse hearts. The SDS gels were stained with Coomassie Blue (R-250, Bio-Rad Laboratories, Hercules, CA). To determine the level of expression of sarcomeric proteins, the band profiles of each protein from the gel were compared between NTG and TG mouse hearts. Other details are provided in the Supporting Material. The phosphorylation status of sarcomeric proteins was assessed by running a 15% SDS-PAGE. The gel was stained with Pro-Q diamond phosphoprotein staining solution (Invitrogen, Carlsbad, CA). The phosphorylation status of sarcomeric proteins in the NTG and TG mouse hearts was assessed by comparing the phosphoprotein-stained band profiles.

Western blot

Muscle protein extracts from NTG and TG mouse cardiac preparations were resolved using 12.5% SDS-PAGE (10). Proteins from the gel were transferred to a PVDF membrane, and cTnT was probed by two antibodies: an anti-cTnT primary (Clone M401134; Fitzgerald Industries International, Concord, MA) and an anti-mouse secondary antibody (Amersham RPN2132, GE Healthcare Biosciences, Pittsburgh, PA). To quantify the relative amount of the chimeric cTnT in the TG mouse heart, densitometric analysis was carried out using the ImageJ software (National Institutes of Health).

Preparation of detergent-skinned cardiac muscle fiber bundles

Detergent-skinned papillary muscle fiber bundles from NTG and TG mouse hearts were prepared as described in the Supporting Material.

pCa solutions

All measurements in this study were conducted at 20°C. The pH of each pCa solution was adjusted to 7.0. The ionic strength of all pCa solutions was 180 mM. The compositions of the relaxing solution (pCa 9.0) and the maximal Ca^{2+}-activating solution (pCa 4.3) at 20°C were as described in the Supporting Material. The reagent concentrations of all pCa solutions were calculated based on the program developed by Fabiato and Fabiato (13).

Simultaneous measurements of isometric steady-state force and ATPase activity

The muscle fiber was attached between a force transducer and a servo motor using aluminum clips. The resting SL was adjusted to 1.9 or 2.3 μm in pCa 9.0 solution via a laser diffraction technique (14). The fiber was then activated with a series of pCa solutions starting from pCa 4.3 to pCa 9.0. Steady-state force and ATPase activity were simultaneously measured in each pCa activation (14). The ATPase activity was measured via a change in the oxidation of NADH, which was linked to enzymatically coupled reactions (14–16). For more details, see the Supporting Material.

Rate of tension redevelopment (k_{tr})

Measurements of k_{tr} were obtained in maximally activated (pCa 4.3) muscle fibers using a slack/restretch protocol as described in the Supporting Material.

Measurement of dynamic muscle fiber stiffness using step-like length perturbations

A series of step-like length perturbations ($\pm$0.5%, 1.0%, 1.5%, and 2.0% of the preset muscle length (ML)) was applied to maximally activated fibers and the force responses were measured (17). Representative traces of various-amplitude quick stretches/quick releases and the corresponding force responses are shown in Fig. 1. A nonlinear recruitment-distortion (NLRD) model was fitted to the data to estimate the following model parameters: the rate by which new strong cross-bridges (XBs) were recruited due to a change in ML (b), the rate by which the strain of stretched XBs was dissipated after a sudden change in ML (c), the instantaneous stiffness as estimated from the initial incident force response to a sudden change in ML (E_D), and the magnitude of increase in stiffness from the initial steady state to the new steady state due to the recruitment of additional XBs (E_R). For more details on the NLRD model formulation and the significance of the model parameters (b, c, E_D, and E_R), please see the Supporting Material.

Measurement of muscle fiber shortening velocity

Force-velocity (F-V) relationships were measured with the use of a force-ramp (F-R) protocol (18). Briefly, a force perturbation was applied on a maximally activated muscle fiber as a linear time-dependent decrease in force i.e., F-R (Fig. 2 *A*). To estimate the maximal shortening velocity, V_{max}, the muscle fiber was allowed to shorten continuously against the force until the force on the fiber was ramped down to near zero (Fig. 2 *B*). Force data were normalized by the isometric steady-state value, F_0, and the shortening velocity by the ML just before perturbation. Normalized force data were plotted against the normalized velocity data to construct the F-V relationship for each fiber (Fig. 2 *C*). V_{max} was estimated as the velocity at which the net force elicited by the fiber was zero (illustrated by the *arrow* in Fig. 2 *C*). All other details are provided in the Supporting Material.

Statistical analysis

A two-way analysis of variance (ANOVA) was used to analyze the data, with the TnT species (native cTnT versus chimeric cTnT) and SL

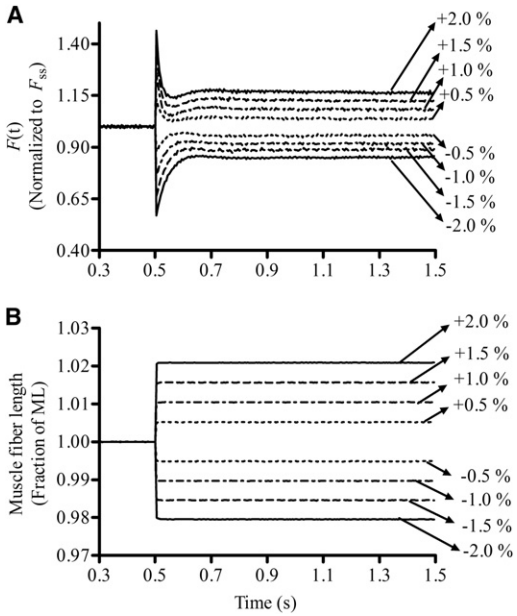

FIGURE 1 Force responses of an NTG muscle fiber to step-like length perturbations. For simplicity and clarity, only the traces of one NTG muscle fiber are shown. (*A*) Force responses of a maximally activated (pCa 4.3) muscle fiber at SL 2.3 μm normalized to isometric steady-state force (F_{ss}). (*B*) Length perturbation refers to the step-like stretch and release of the muscle fiber by $\pm 0.5\%$, $\pm 1.0\%$, $\pm 1.5\%$, and $\pm 2.0\%$ of the initial ML. See the Supporting Material for details.

(1.9 μm vs. 2.3 μm) used as the two factors. When the differences between effects of native cTnT versus chimeric cTnT were dissimilar at different SLs, the interaction effect became significant. When the interaction effect was significant, it suggested that the effect of cTnT on a given contractile parameter depended on SL. When the interaction effect was not significant, only the main effect was interpreted. When the main effect was significant, the difference between effects of native cTnT versus chimeric cTnT on a contractile parameter showed a similar trend at both SLs. When appropriate, post hoc multiple comparisons were made using Holm-Bonferroni corrected *t*-tests to compare the effects of TnT at a given SL (19).

RESULTS

Chimeric cTnT: replacement of 1-73 amino acids of McTnT with 1-41 residues of MfsTnT

The rationale for making this chimeric cTnT is as follows: The significance of the N-terminal end region of McTnT can be categorized based on the amino acid sequence, the length of the amino acid chain, and the net negative charge (Fig. 3 *A*). An aligned sequence comparison of 1–103 residues of McTnT and 1–71 residues of MfsTnT using the LALIGN program (20) reveals that 1), McTnT is 32 amino acids longer at the N-terminal end; 2), there is 57.5% sequence heterogeneity between the two proteins; and 3), the N-terminal end of McTnT has a higher net negative charge, and thus is more acidic than that of MfsTnT (a net charge of −20 vs. −30 in McTnT). The fact that the NTE of cTnT is highly conserved in hearts of different species (1) suggests that it has a heart-specific functional role (Fig. 3 *B*).

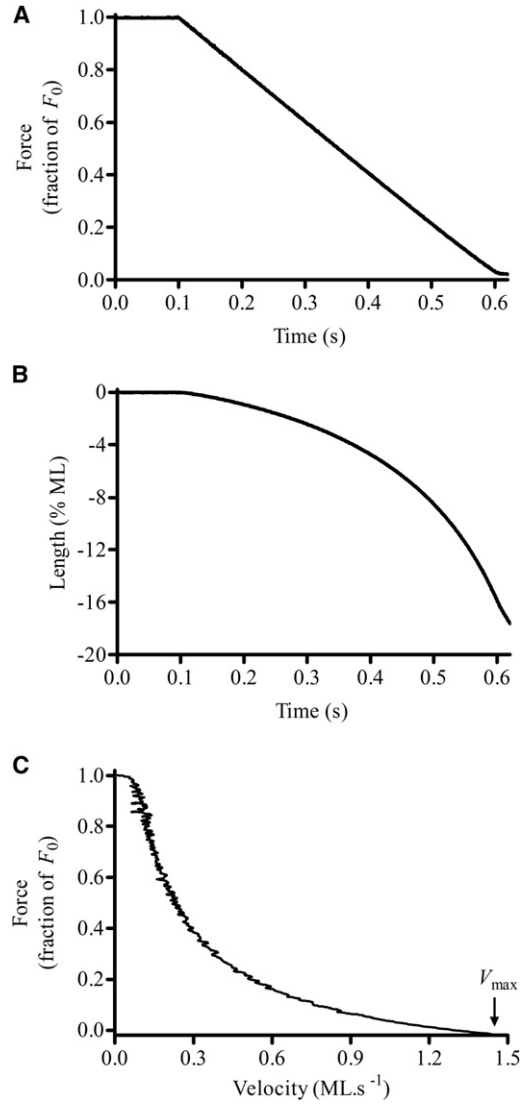

FIGURE 2 Measurement of the F-V relationship. (*A*) Representative sample of F-R perturbation in a NTG cardiac muscle fiber at an SL of 2.3 μm. The ramp rate was set to -2.0 F_0/s, where F_0 is the initial steady-state isometric force. (*B*) ML changes corresponding to the imposed loads on muscle fiber shown in panel *A*. Velocity was estimated by taking the ratio of change in ML to change in time. (*C*) F-V relationship. Measured force values were normalized with the initial force, F_0, and velocities were normalized with the initial ML just before force perturbation. Normalized force data were plotted against normalized velocity data to construct the F-V relationship. V_{max} was estimated by fitting the Hill's hyperbolic F-V relationship to the experimentally determined F-V data (indicated by the *arrow*). For additional details, please see the Supporting Material.

Expression level and phosphorylation status of sarcomeric proteins in TG mouse hearts

In comparison with their NTG mouse littermates, the TG mice appeared normal and showed no evidence of increased morbidity or phenotypic differences. The heart weight/body weight ratio, and the size of TG mouse hearts were similar to those of NTG mouse hearts. Fig. S1 demonstrates that the

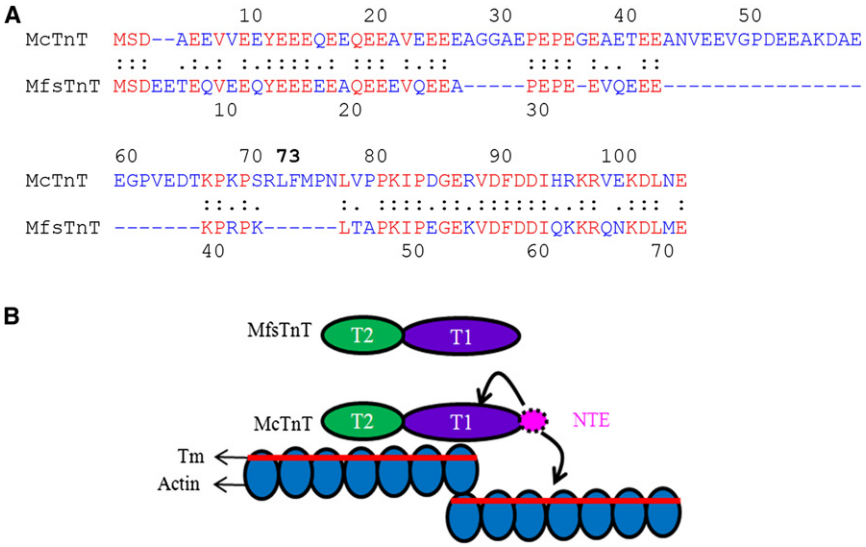

FIGURE 3 Comparison of the N-terminal ends of McTnT and MfsTnT. (*A*) The LALIGN program (20) was used to compare the N-terminal ends of McTnT and MfsTnT. The "." indicates conservative replacement, ":" indicates identity, " " indicates nonconservative replacement, and "-" indicates deletion introduced to maximize sequence similarities. The amino acids in red represent identical replacements, and all other replacements are indicated in blue. (*B*) A cartoon of the thin-filament structure highlighting the position of the cardiac NTE in cTnT. The T1 and T2 domains of McTnT and MfsTnT are shown by purple and green, respectively. The NTE of McTnT is shown in pink. Curved arrows indicate possible sites of action of the NTE on cardiac thin filaments.

total expression level of each sarcomeric protein did not differ between NTG and TG mouse hearts. Furthermore, the phosphorylation status of all major sarcomeric proteins, including cTnT, was also not affected in TG mouse hearts (Fig. S2).

Expression of chimeric cTnT in TG mouse hearts

The Western blot profile of TG mouse cardiac muscle preparations shown in Fig. 4 demonstrates the presence of both native and chimeric cTnT proteins (lane 2). Estimates made from a densitometric analysis of the protein profiles reveal that the level of expression of chimeric cTnT is ~54% (of the total) in TG mouse hearts.

Effect of chimeric cTnT on Ca^{2+}-activated maximal tension and ATPase activity

A comparison of Ca^{2+}-activated maximal tension and ATPase activity from detergent-skinned NTG and TG fibers revealed no significant differences at both short and long SLs. Maximal tensions (in $mN.mm^{-2}$) in NTG and TG fibers at short SL were respectively 29 ± 1 and 30 ± 1 at short SL, and 47 ± 2 and 46 ± 2 at long SL. The corresponding maximal ATPase activities (in $pmol.mm^{-3}.s^{-1}$) at short SL were 323 ± 20 and 320 ± 12 at short SL, and 314 ± 11 and 294 ± 7 at long SL. Thus, the effects of the TnT species-SL interaction on maximal tension and ATPase activity were not significant. These observations indicate that the chimeric cTnT had no effect on maximal tension or ATPase activity at either SL. In other words, the absence of the NTE did not affect Ca^{2+}-activated maximal tension or ATPase activity.

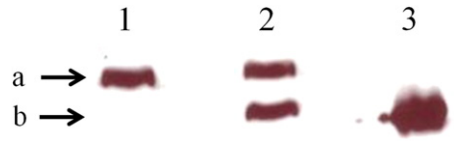

FIGURE 4 Western blot analysis. NTG and TG cardiac muscle preparations were run on a 12.5% SDS-PAGE. An anti-cTnT primary antibody and an anti-mouse secondary antibody were used to detect native cTnT and chimeric cTnT. Lane 1: NTG cardiac muscle; lane 2: TG cardiac muscle; lane 3: chimeric cTnT standard. (*a*) Native cTnT. (*b*) Chimeric cTnT. ImageJ software was used to scan the band intensities in different lanes. The total optical band intensity (i.e., the total amount of cTnT expressed) in TG cardiac mouse hearts (lane 2) was assumed to be the sum of the optical band intensities of native cTnT and chimeric cTnT protein profiles. The expression level of the chimeric cTnT was determined by dividing the optical band intensity of the chimeric cTnT protein profile by the total band intensity, which was measured to be ~54%.

Effect of chimeric cTnT on myofilament Ca^{2+} sensitivity (pCa_{50}) and cooperativity (n_H)

To estimate pCa_{50} and n_H, the Hill's equation was fitted to pCa-tension relationships at short (Fig. 5 *A*) and long (Fig. 5 *B*) SLs. When compared with NTG fibers, the pCa-tension relationships of TG fibers showed a leftward shift by 0.34 pCa units at both SLs (Fig. 5, *A* and *B*). The effect of the TnT species-SL interaction on pCa_{50} was not significant, but the main effect due to TnT species was significant ($p < 0.001$). When the pCa values were converted into micromolar concentrations using the equation pCa = -log of $[Ca^{2+}]_{free}$, a shift of 0.34 pCa units corresponded to a ~2.2-fold increase in the Ca^{2+} sensitivity of TG fibers at both SLs. In other words, the TG fibers required 2.2-fold lower Ca^{2+} concentrations to produce the same amount of tension as the NTG fibers (Fig. 5 *C*). Because the SL-dependent increase in pCa_{50} was identical in both groups (0.14 in NTG and TG fibers), the chimeric cTnT (or the absence of the NTE) had no impact on the length-mediated effects on pCa_{50}. There was no significant change in n_H of TG fibers at short SL, but there was a significant decrease at long SL ($p < 0.05$; Fig. 5 *D*). Thus, the effect

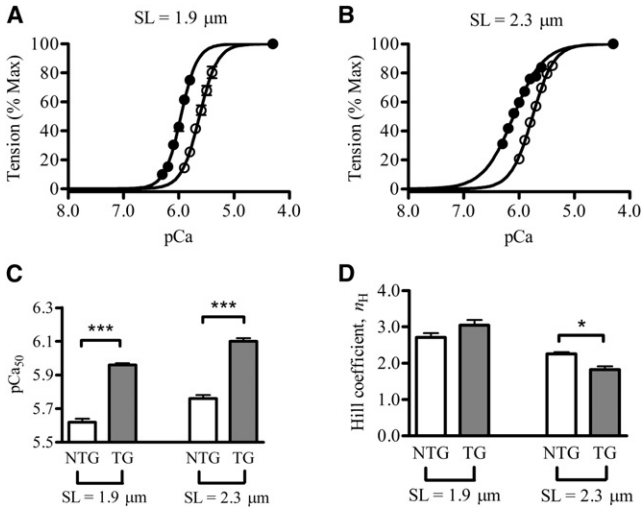

FIGURE 5 Normalized pCa-tension relationships at (*A*) SL 1.9 μm and (*B*) SL 2.3 μm. Tension values were normalized with respect to the maximal value at pCa 4.3. ○, NTG fibers; ●, TG fibers. The Hill equation was fitted to pCa-tension data to derive myofilament Ca^{2+} sensitivity (pCa_{50}) and cooperativity (n_H). Data were analyzed by two-way ANOVA. (*C*) Effect of SL on pCa_{50}. The main effect was significant (***$p < 0.001$), suggesting that the chimeric cTnT-induced increase in pCa_{50} of TG fibers was similar at both SLs. (*D*) Effect of SL on n_H. The interaction effect was significant ($p < 0.01$), suggesting that the effect of the chimeric cTnT depended on SL. Post hoc multiple comparisons suggested that the chimeric cTnT had a significant (*$p < 0.05$) impact on cooperativity at SL of 2.3 μm, but not at 1.9 μm. Values are expressed as the mean ± SE. The number of determinations was at least nine in each group. Statistical significance was set at $p < 0.05$.

of the TnT species-SL interaction on n_H was significant ($p < 0.01$). This observation suggests that the chimeric cTnT had a significant impact on myofilament cooperativity at long SL. pCa-ATPase relationships were also measured in NTG and TG fibers, and Hill's equation was fitted to these data to estimate pCa_{50} and n_H. When compared with the NTG fiber data at both SLs, the effects of the pCa-ATPase relationships in the TG fibers were similar to those of the pCa-tension relationships, as shown by the corresponding estimates of pCa_{50} and n_H (Table S1).

Effect of chimeric cTnT on XB turnover rate

To assess whether the chimeric cTnT affected the XB turnover rate, we estimated the rate of tension redevelopment (k_{tr}) and the rate of length-mediated XB recruitment (b) at short and long SLs (see Materials and Methods). Previous studies have shown that k_{tr} is a valuable index of the XB turnover rate (21) and that it correlates with b (15). At maximal activation (pCa 4.3), the k_{tr} estimates from TG fibers were similar to those of NTG fibers at both SLs (Table 1). Our approximations of b also showed no significant differences between NTG and TG fibers (Table 1). Thus, the chimeric cTnT had no impact on the length-mediated effects on either maximal k_{tr} or b.

TABLE 1 Effects of the chimeric cTnT on various contractile function and mechano-dynamic parameters

SL	Model parameter	NTG	TG
Cross-bridge turnover kinetics			
1.9 μm	k_{tr} (s^{-1})	12.25 ± 1.06	13.02 ± 0.83
	b (s^{-1})	26.52 ± 1.80	27.78 ± 3.29
2.3 μm	k_{tr} (s^{-1})	10.95 ± 0.43	10.80 ± 1.06
	b (s^{-1})	28.60 ± 1.03	25.26 ± 3.39
Muscle fiber stiffness parameters			
1.9 μm	E_D ($mN \cdot mm^{-3}$)	763.15 ± 45.82	779.01 ± 52.96
	E_R ($mN \cdot mm^{-3}$)	131.82 ± 7.98	125.35 ± 7.99
2.3 μm	E_D ($mN \cdot mm^{-3}$)	904.65 ± 43.33	989.29 ± 51.78
	E_R ($mN \cdot mm^{-3}$)	232.41 ± 20.24	277.69 ± 33.05
Cross-bridge detachment kinetics			
1.9 μm	TC ($pmol \cdot mN^{-1} \cdot mm^{-1} \cdot s^{-1}$)	11.89 ± 0.87	10.62 ± 0.30
	c (s^{-1})	49.33 ± 5.67	49.92 ± 6.45
	V_{max} ($ML \cdot s^{-1}$)	1.25 ± 0.04	1.21 ± 0.05
2.3 μm	TC ($pmol \cdot mN^{-1} \cdot mm^{-1} \cdot s^{-1}$)	7.12 ± 0.26	6.37 ± 0.26
	c (s^{-1})	40.22 ± 2.36	32.08 ± 3.89
	V_{max} ($ML \cdot s^{-1}$)	1.40 ± 0.05	1.41 ± 0.05

Parameters b, c, E_D, and E_R were estimated using the nonlinear recruitment-distortion model (17), and k_{tr} was determined by using a large release-restretch protocol (32). The TC was determined as described previously (15,36). V_{max} was estimated using the F-V relationships (18). See the Supporting Material for details on the experimental approaches. NTG and TG refer to nontransgenic and transgenic fibers, respectively. Two-way ANOVA was used to analyze the data. No significant differences were observed between NTG and TG fibers in any of the parameter estimates listed in this table. Values are expressed as the mean ± SE. The number of determinations was at least nine in each group. Statistical significance was set at $p < 0.05$.

We also measured the effects of the chimeric cTnT on k_{tr} at submaximal Ca^{2+} activation. We selected two pCa levels at short SL (pCa 5.7 and 5.9) and two at long SL (pCa 5.8 and 6.0). The rationale for choosing these pCa levels is as follows: n_H is more prominent at submaximal Ca^{2+} activation, which in turn has a significant impact on k_{tr}. For NTG fibers, we chose a value of 5.7, which is close to the pCa_{50} of 5.62 in NTG fibers. For TG fibers, we chose a value of 5.9, which is close to the pCa_{50} of 5.96 in TG fibers (at SL 1.9 μm). A similar argument applies for our choice of pCa levels at SL 2.3 μm. Submaximally activated TG fibers demonstrated no significant effects on k_{tr} estimates at short SL (Table 2). This observation is consistent with our finding that n_H of TG fibers is not significantly different from that of NTG fibers at short SL (Fig. 5 *D*). However, k_{tr} estimates in TG fibers increased significantly ($p < 0.01$) at long SL. This increase amounted to ~52% and 92% at pCa of 5.8 and 6.0, respectively (Table 2). These observations demonstrate that a significant decrease in n_H of TG fibers at long SL (Fig. 5 *D*) caused a significant increase in k_{tr} at submaximal Ca^{2+} levels (Table 2).

TABLE 2 Effects of the chimeric cTnT on the rate of tension redevelopment (k_{tr}) at submaximal Ca^{2+} activations

SL	pCa	NTG k_{tr} (s^{-1})	TG k_{tr} (s^{-1})
1.9 μm	5.7	6.90 ± 0.18	7.62 ± 0.17
	5.9	1.85 ± 0.08	2.15 ± 0.07
2.3 μm	5.8	5.16 ± 0.16	7.86 ± 0.26**
	6.0	1.58 ± 0.03	3.01 ± 0.10***

We determined k_{tr} using a large release-restretch protocol (32). The pCa levels chosen at short SL (1.9 μm) and long SL (2.3 μm) correspond to submaximal Ca^{2+} levels for NTG and TG fibers, respectively. NTG and TG refer to nontransgenic and transgenic fibers, respectively. One-way ANOVA was used to analyze k_{tr} estimates. Values are expressed as the mean ± SE. The number of determinations was at least five in each group. $^{**}p < 0.01$; $^{***}p < 0.001$.

Effect of chimeric cTnT on the muscle fiber stiffness parameters (E_D and E_R)

To investigate whether the chimeric cTnT affected the magnitude of XB recruitment and distortion dynamics, we estimated ML-mediated stiffness parameters (E_D and E_R) using the force responses of the fibers to step-like length perturbations (for more information on how E_D and E_R were estimated, please see "NLRD model formulation", "Characteristic features of force responses to step-like length perturbations", and Fig. S5 in the Supporting Material). Our estimates of E_D and E_R from TG fibers showed no significant differences when compared with those obtained from NTG fibers (Table 1). Our findings on E_R suggest that the length-mediated increase in the number of strong XBs was not affected by the chimeric cTnT (or the absence of the NTE). Similar findings were also observed in E_D, demonstrating that the number of strongly bound XBs was also not affected by the chimeric cTnT.

Effect of chimeric cTnT on XB detachment kinetics

To investigate whether the XB detachment kinetics was affected by the chimeric cTnT, we measured tension cost (TC), XB distortion rate constant (c), and maximal muscle fiber shortening velocity (V_{max}) in NTG and TG fibers at short and long SLs. TC was estimated using methods described elsewhere (14,22), and was previously shown to be useful for approximating the XB detachment rate, g (23). Our TC measurements showed no significant differences between NTG and TG fibers at both SLs (Table 1). Our estimates of the length-mediated XB distortion dynamic, c, also showed no significant differences between NTG and TG fibers at both SLs (Table 1). In a previous work, we showed that TC is strongly correlated to c (24). Thus, similar effects observed in c and TC support the notion that the XB detachment kinetics is not affected by the chimeric cTnT (or the absence of the NTE). This is further substantiated by our estimates of V_{max}, which is known to be strongly influenced by g (25). The V_{max} estimates showed no significant differences between NTG and TG fibers at both SLs (Table 1). Thus, the NTE of cTnT does not affect the XB detachment kinetics.

DISCUSSION

The biological significance of the 32 amino acid NTE in cTnT remains unknown. Given the highly conserved nature of the NTE in hearts of different species, we hypothesized that the NTE has a unique regulatory role in cardiac myofilament activation. Assuming a straight α-helix, 32 amino acids in McTnT would translate to an additional ~48 Å in length (2) as compared with MfsTnT (Fig. 3 *B*). Our understanding of the structure of the thin filament, based on studies of fast skeletal muscle, suggests that the N-terminus of cTnT extends ~12% into the neighboring regulatory unit (RU; Tm-Tn). In this first (to our knowledge) explicit study of the NTE of cTnT, we used a TG mouse model that expressed a recombinant chimeric cTnT, in which 1–73 amino acids in McTnT were replaced with the corresponding 1–41 residues of MfsTnT. New findings from our study demonstrate that the NTE of cTnT modulates the blocked-to-closed-state transition of the thin filament via its impact on allosteric/cooperative mechanisms.

Myofilament Ca^{2+} sensitivity and cooperativity of tension were altered by the chimeric cTnT

Our measurements of the contractile function and dynamic stiffness parameters in detergent-skinned cardiac muscle fibers from TG mouse hearts resulted in novel (to our knowledge) findings. Our data demonstrate that myofilament Ca^{2+} sensitivity of tension increases dramatically by ~2.2-fold (Fig. 5 *C*) in TG fibers at both short and long SLs. However, the Ca^{2+}-activated maximal tension was not altered by the chimeric cTnT. The uniqueness of our TG mouse model enabled us to attribute the differences in contractile function directly to the NTE. To determine whether this increase in Ca^{2+} sensitivity was due to an increase in the number of strongly bound XBs or due to the length-mediated effect on thin-filament activation, we measured the SL-mediated effect on stiffness parameters (E_D and E_R) in NTG and TG fibers. E_D and E_R represent the magnitudes of the stiffness due to the strain of strongly bound XBs and the length-mediated increase in the number of strong XBs, respectively. Because E_D and E_R in TG fibers are unaffected at both SLs (Table 1), changes in myofilament Ca^{2+} sensitivity can be directly correlated to the NTE-induced effect on thin-filament activation.

One possible clue as to how the chimeric cTnT might affect myofilament Ca^{2+} sensitivity is provided by previous in vitro biochemical studies that used chymotryptic digested products of bovine cTnT (26) and rabbit fsTnT (27). These

proteolytic products (T1 fragments) differed significantly at their N-terminal ends. Observations made from those in vitro biochemical studies suggest that cardiac T1 (cT1) and fast skeletal T1 (fsT1) fragments modulate the regulatory actions of Tm on thin-filament states in different ways, that is, fsT1 favors the stabilization of the closed state and cT1 favors the stabilization of the blocked state. Therefore, a logical interpretation of these in vitro studies is that the chimeric cTnT, which lacks the cardiac-specific NTE, may have favored the transition of the thin filament from the blocked to the closed state, thus increasing myofilament Ca^{2+} sensitivity in TG muscle fibers. Previous studies have shown that sequence alterations in the N-terminus affect the net charge of the cTnT molecule, rendering it either acidic or basic. A shift of the TnT isoform from an acidic to a basic form was previously shown to promote strong TnT-Tm interactions, resulting in an increase in the thin-filament cooperativity (8,10). On the other hand, studies that measured the binding affinities of TnT to Tm demonstrated a rigid TnT-Tm coupling (4,5), which suggests a decrease in the thin-filament activation through a negative impact on cooperative interaction between two contiguous RU. In our study, the Hill coefficient (n_H) values of normalized pCa-tension relationships were significantly lower in TG fibers at SL 2.3 μm (Fig. 5 *D*). Such a drop in n_H is consistent with a decrease in the cooperativity of thin filaments. However, no differences observed in n_H of TG fibers at SL 1.9 μm suggest that the effect of chimeric cTnT on Tm may vary significantly with SL. Although we do not fully comprehend how the SL modulates thin-filament cooperativity (28), some data suggest that the SL-mediated effects on myofilament kinetics vary with the SL (15,29). Thus, the different effects of the chimeric cTnT on myofilament cooperativity at different SLs warrant further investigation.

XB detachment kinetics were not altered by the chimeric cTnT

One of the mechanisms by which the chimeric cTnT could affect myofilament Ca^{2+} sensitivity or cooperativity would be to alter the XB detachment kinetics. Because previous studies have shown that TnT isoforms influence XB detachment kinetics (15,17), we wanted to determine whether the XB detachment rate was altered in TG fibers. Estimates of TC and the length-mediated XB distortion dynamic, c, demonstrated that the XB detachment kinetics remained unaltered in TG fibers. This is further substantiated by our estimates of V_{max} in NTG and TG fibers. The range of V_{max} values obtained from NTG mouse fibers in this study (Table 1) are within the range of values reported in earlier studies (30,31). No statistical significance observed in V_{max} estimates between NTG and TG fibers correlated well with similar trends in TC and the distortion rate constant, c (Table 1).

Maximal XB turnover rate was not altered by the chimeric cTnT

To account for an increased Ca^{2+} sensitivity of tension in TG fibers, we expect an increase in the number of RUs that are turned on during submaximal activation. Thus, the effect of chimeric cTnT on the Ca^{2+} sensitivity of tension appears to be exerted via its effect on the thin filaments, and more precisely on the Ca^{2+}-mediated transition between the blocked and closed states (26,27), rather than through changes in the intrinsic XB cycling rate. Our measurements of k_{tr} and XB detachment kinetics (see above) at maximal Ca^{2+} activation support this argument because k_{tr} is determined by the sum of f and g (15). Because k_{tr} is a measure of the XB transition rate from a weak binding state to a strong one (32,33), a change in k_{tr} could be attributed to an effect on the equilibrium between the closed and open states of thin filaments (33). Measurements of k_{tr} at maximal Ca^{2+} activation demonstrate that k_{tr} in TG fibers remained unaltered (Table 1). In conjunction with previous findings regarding the effect of cT1 on the blocked state of thin filaments (26), our study suggests that the transition of cardiac thin filament from the blocked to the closed state is affected by the chimeric cTnT. We predict that the chimeric cTnT exerts its effect by modulating cooperative mechanisms in the thin filament. Based on decreased cooperativity in TG fibers at long SL, Campbell's modified two-state model (33) would predict that at submaximal levels of Ca^{2+}, k_{tr} of TG fibers would be significantly higher than that of NTG fibers, because the initial condition (cooperative effects) from which force redevelopment takes place is altered in TG fibers. As expected, k_{tr} values of TG fibers at SL 2.3 μm were substantially higher than those of NTG fibers at pCa 5.8 and 6.0 (52% and 92%, respectively; Table 2). Therefore, changes in cooperative effects that exist at the onset of force redevelopment must result from an effect of chimeric cTnT on the thin filament.

CONCLUSION

Our study provides valuable insight into the mechanism by which the unique NTE of cTnT affects Ca^{2+}-mediated regulation of cardiac myofilaments. Because the NTE of cTnT has major effects on the dynamics of strong TnT-Tm interactions (2), our data provide mechanistic understanding of how the NTE of cTnT modulates Ca^{2+}-activation of cardiac thin filaments. Through its effect on either the Tm-Tm overlapping ends or the near-neighbor RU (indicated by curved arrows in Fig. 3 *B*), the NTE may affect allosteric/cooperative mechanisms within the thin filament in such a way that the Ca^{2+}-mediated transition from the blocked to the closed state is altered. Our observation has significant implications for understanding the functional differences due to tissue-specific expression of TnT isoforms. Because

functionally distinct cTnT isoforms that differ primarily in their N-terminal end regions are variably expressed during developmental regulation and cardiomyopathy (1,34,35), our study also has significant implications for age- and disease-related changes in the expression of cTnT isoforms in the human heart.

SUPPORTING MATERIAL

Materials and methods, a table, five figures, and references (36–41) are available at http://www.biophysj.org/biophysj/supplemental/S0006-3495(12)00848-X.

We thank Dr. Mariappan Muthuchamy (Texas A&M University) for help in generating TG mice.

This work was supported by National Institutes of Health grant HL-075643 to M.C. and Poncin Scholarship to R.M.

REFERENCES

1. Wei, B., and J. P. Jin. 2011. Troponin T isoforms and posttranscriptional modifications: evolution, regulation and function. *Arch. Biochem. Biophys.* 505:144–154.
2. Perry, S. V. 1998. Troponin T: genetics, properties and function. *J. Muscle Res. Cell Motil.* 19:575–602.
3. Jin, J. P., Z. Zhang, and J. A. Bautista. 2008. Isoform diversity, regulation, and functional adaptation of troponin and calponin. *Crit. Rev. Eukaryot. Gene Expr.* 18:93–124.
4. Biesiadecki, B. J., S. M. Chong, …, J. P. Jin. 2007. Troponin T core structure and the regulatory NH2-terminal variable region. *Biochemistry.* 46:1368–1379.
5. Chandra, M., D. E. Montgomery, …, R. J. Solaro. 1999. The N-terminal region of troponin T is essential for the maximal activation of rat cardiac myofilaments. *J. Mol. Cell. Cardiol.* 31:867–880.
6. Communal, C., M. Sumandea, …, R. J. Hajjar. 2002. Functional consequences of caspase activation in cardiac myocytes. *Proc. Natl. Acad. Sci. USA.* 99:6252–6256.
7. Sumandea, M. P., S. Vahebi, …, E. Homsher. 2009. Impact of cardiac troponin T N-terminal deletion and phosphorylation on myofilament function. *Biochemistry.* 48:7722–7731.
8. Huang, Q. Q., F. V. Brozovich, and J. P. Jin. 1999. Fast skeletal muscle troponin T increases the cooperativity of transgenic mouse cardiac muscle contraction. *J. Physiol.* 520:231–242.
9. MacFarland, S. M., J. P. Jin, and F. V. Brozovich. 2002. Troponin T isoforms modulate calcium dependence of the kinetics of the cross-bridge cycle: studies using a transgenic mouse line. *Arch. Biochem. Biophys.* 405:241–246.
10. Montgomery, D. E., M. Chandra, …, R. J. Solaro. 2001. Transgenic incorporation of skeletal TnT into cardiac myofilaments blunts PKC-mediated depression of force. *Am. J. Physiol. Heart Circ. Physiol.* 280:H1011–H1018.
11. Muthuchamy, M., I. L. Grupp, …, D. F. Wieczorek. 1995. Molecular and physiological effects of overexpressing striated muscle beta-tropomyosin in the adult murine heart. *J. Biol. Chem.* 270:30593–30603.
12. Walter, C. A., D. Nasr-Schirf, and V. J. Luna. 1989. Identification of transgenic mice carrying the CAT gene with PCR amplification. *Biotechniques.* 7:1065–1070.
13. Fabiato, A., and F. Fabiato. 1979. Calculator programs for computing the composition of the solutions containing multiple metals and ligands used for experiments in skinned muscle cells. *J. Physiol. (Paris).* 75:463–505.
14. de Tombe, P. P., and G. J. Stienen. 1995. Protein kinase A does not alter economy of force maintenance in skinned rat cardiac trabeculae. *Circ. Res.* 76:734–741.
15. Chandra, M., M. L. Tschirgi, …, K. B. Campbell. 2006. Troponin T modulates sarcomere length-dependent recruitment of cross-bridges in cardiac muscle. *Biophys. J.* 90:2867–2876.
16. Stienen, G. J., R. Zaremba, and G. Elzinga. 1995. ATP utilization for calcium uptake and force production in skinned muscle fibres of Xenopus laevis. *J. Physiol.* 482:109–122.
17. Ford, S. J., M. Chandra, …, K. B. Campbell. 2010. Model representation of the nonlinear step response in cardiac muscle. *J. Gen. Physiol.* 136:159–177.
18. Lin, D. C., and T. R. Nichols. 2003. Parameter estimation in a cross-bridge muscle model. *J. Biomech. Eng.* 125:132–140.
19. Glantz, S. A. 2002. Primer of Biostatistics. McGraw-Hill, New York.
20. Huang, X., and W. Miller. 1991. A time-efficient, linear-space local similarity algorithm. *Adv. Appl. Math.* 12:337–357.
21. Brenner, B. 1988. Effect of Ca^{2+} on cross-bridge turnover kinetics in skinned single rabbit psoas fibers: implications for regulation of muscle contraction. *Proc. Natl. Acad. Sci. USA.* 85:3265–3269.
22. Chandra, M., M. L. Tschirgi, and J. C. Tardiff. 2005. Increase in tension-dependent ATP consumption induced by cardiac troponin T mutation. *Am. J. Physiol. Heart Circ. Physiol.* 289:H2112–H2119.
23. de Tombe, P. P., and G. J. Stienen. 2007. Impact of temperature on cross-bridge cycling kinetics in rat myocardium. *J. Physiol.* 584: 591–600.
24. Campbell, K. B., M. Chandra, …, W. C. Hunter. 2004. Interpreting cardiac muscle force-length dynamics using a novel functional model. *Am. J. Physiol. Heart Circ. Physiol.* 286:H1535–H1545.
25. Huxley, A. F. 1957. Muscle structure and theories of contraction. *Prog. Biophys. Biophys. Chem.* 7:255–318.
26. Tobacman, L. S., M. Nihli, …, E. Homsher. 2002. The troponin tail domain promotes a conformational state of the thin filament that suppresses myosin activity. *J. Biol. Chem.* 277:27636–27642.
27. Maytum, R., M. A. Geeves, and S. S. Lehrer. 2002. A modulatory role for the troponin T tail domain in thin filament regulation. *J. Biol. Chem.* 277:29774–29780.
28. Moss, R. L., and D. P. Fitzsimons. 2002. Frank-Starling relationship: long on importance, short on mechanism. *Circ. Res.* 90:11–13.
29. Adhikari, B. B., M. Regnier, …, D. A. Martyn. 2004. Cardiac length dependence of force and force redevelopment kinetics with altered cross-bridge cycling. *Biophys. J.* 87:1784–1794.
30. Korte, F. S., K. S. McDonald, …, R. L. Moss. 2003. Loaded shortening, power output, and rate of force redevelopment are increased with knockout of cardiac myosin binding protein-C. *Circ. Res.* 93:752–758.
31. Miller, M. S., B. M. Palmer, …, D. W. Maughan. 2005. The essential light chain N-terminal extension alters force and fiber kinetics in mouse cardiac muscle. *J. Biol. Chem.* 280:34427–34434.
32. Brenner, B., and E. Eisenberg. 1986. Rate of force generation in muscle: correlation with actomyosin ATPase activity in solution. *Proc. Natl. Acad. Sci. USA.* 83:3542–3546.
33. Campbell, K. 1997. Rate constant of muscle force redevelopment reflects cooperative activation as well as cross-bridge kinetics. *Biophys. J.* 72:254–262.
34. Anderson, P. A., N. N. Malouf, …, P. D. Allen. 1991. Troponin T isoform expression in humans. A comparison among normal and failing adult heart, fetal heart, and adult and fetal skeletal muscle. *Circ. Res.* 69:1226–1233.
35. Gomes, A. V., G. Guzman, …, J. D. Potter. 2002. Cardiac troponin T isoforms affect the Ca^{2+} sensitivity and inhibition of force development. Insights into the role of troponin T isoforms in the heart. *J. Biol. Chem.* 277:35341–35349.

36. Chandra, M., V. L. Rundell, …, R. J. Solaro. 2001. Ca(2+) activation of myofilaments from transgenic mouse hearts expressing R92Q mutant cardiac troponin T. *Am. J. Physiol. Heart Circ. Physiol.* 280:H705–H713.

37. Chandra, M., M. L. Tschirgi, …, K. B. Campbell. 2007. Interaction between myosin heavy chain and troponin isoforms modulate cardiac myofiber contractile dynamics. *Am. J. Physiol. Regul. Integr. Comp. Physiol.* 293:R1595–R1607.

38. Laemmli, U. K. 1970. Cleavage of structural proteins during the assembly of the head of bacteriophage T4. *Nature.* 227:680–685.

39. Linari, M., R. Bottinelli, …, V. Lombardi. 2004. The mechanism of the force response to stretch in human skinned muscle fibres with different myosin isoforms. *J. Physiol.* 554:335–352.

40. Stelzer, J. E., and R. L. Moss. 2006. Contributions of stretch activation to length-dependent contraction in murine myocardium. *J. Gen. Physiol.* 128:461–471.

41. Hill, A. V. 1938. The heat of shortening and the dynamic constants of muscle. *Proc. R. Soc. Lond. B Biol. Sci.* 126:136–195.